



Formation of Metastable Disordered Ni₃Al by Pulsed Laser-Induced Rapid Solidification

Citation

West, Jeffrey A., James T. Manos, and Michael J. Aziz. 1991. Formation of metastable disordered Ni₃Al by pulsed laser-induced rapid solidification. Materials Research Society Symposia Proceedings 213: 859-864.

Published Version

http://www.mrs.org/s_mrs/sec.asp?CID=1727&DID=38980

Permanent link

<http://nrs.harvard.edu/urn-3:HUL.InstRepos:2870604>

Terms of Use

This article was downloaded from Harvard University's DASH repository, and is made available under the terms and conditions applicable to Other Posted Material, as set forth at <http://nrs.harvard.edu/urn-3:HUL.InstRepos:dash.current.terms-of-use#LAA>

Share Your Story

The Harvard community has made this article openly available.
Please share how this access benefits you. [Submit a story](#).

[Accessibility](#)

FORMATION OF METASTABLE DISORDERED Ni_3Al BY PULSED LASER-INDUCED RAPID SOLIDIFICATION

Jeffrey A. West, James T. Manos, and Michael J. Aziz,
Division of Applied Sciences, Harvard University, Cambridge, MA 02138.

ABSTRACT

Thin films of Ni_3Al formed by co-evaporation onto insulating substrates form a single phase fcc disordered lattice upon rapid solidification following excimer laser-induced melting with an interface velocity of ~ 4 m/s. Transmission Electron Microscopy (TEM) and x-ray diffraction (XRD) analyses exhibit no superlattice diffraction at room temperature. Resistivity measurements, indicating that the disordered phase has a higher resistivity and much smaller temperature coefficient at room temperature than the stable ordered (L_{12}) phase, permit us to monitor phase changes and ordering on a fast time-scale. Subsequent annealing recovers long-range order, with resistivity measurements indicating that reordering begins just below 300°C .

INTRODUCTION

Stable up to its melting point [1], the equilibrium ordered L_{12} (γ') phase of the stoichiometric intermetallic compound Ni_3Al , while ductile as a single crystal, is brittle in its polycrystalline form [2,3]. Useful as a high temperature, high-strength, corrosion-resistant material, this intermetallic would be more practical if a ductile, metastable disordered material existed which was less difficult to machine at room temperature and could be subsequently annealed into the γ' phase. A kinetic model for disorder trapping by Boettinger and Aziz [4] predicts the existence of a critical velocity of a solid-liquid interface beyond which solidification of the metastable disordered phase occurs. Recent attempts to produce a disordered state from the melt by melt-spinning, though unsuccessful, have produced an ordered solid with a long-range order parameter lower than the expected equilibrium value [5]. A completely disordered fcc lattice which remains metastable at room temperature was achieved by adding Fe to the binary alloy. Atomization of stoichiometric Ni_3Al , in which high pressure argon expels liquid from a fine nozzle, induces a quench rate greater than 10^4 K/sec and results in solidification of a disordered state (and often includes some nucleation of the β phase), but undergoes solid-state ordering during cooling from the melting temperature [6]. Here we report the use of the extremely high quench rate attainable by pulsed laser-induced melting of thin films to induce the intermetallic compound Ni_3Al to solidify as a single phase, metastable disordered (γ phase) that persists at room temperature.

Because the electrical resistivity is sensitive to the local atomic arrangement, application of the Transient Conductance Measurement (TCM) technique [7] provides an estimate of the solidification velocity and allows a convenient time-resolved characterization of the solidifying phase from its nucleation at high temperature through the quench to room temperature. Confirmation of the observed γ phase was performed by XRD analysis and TEM diffraction. Subsequent annealing of the disordered phase recovers the ordered phase with ordering beginning just below 300°C ,

as deduced from anomalous changes in resistivity. This is consistent with previous observations of ordering for Ni_3Al which had been disordered by methods other than solidification from the melt [8-10].

EXPERIMENTAL PROCEDURE

Sample Preparation

Thin films (1500Å) of the intermetallic compound Ni_3Al were created by electron-beam co-evaporation of separate nickel (99.9%) and aluminum (99.99%) sources onto a thin (80Å) layer of chromium which was ion-stitched [11] onto a 1.0 μm insulating layer of SiO_2 , created by thermal oxidation of a $\langle 110 \rangle$ oriented Si wafer. The Cr "nucleation layer," which has a melting temperature 470° higher than that of the overlying intermetallic ($\sim 1385^\circ\text{C}$), provides "easy" nucleation sites for solidification of the liquid once the liquid film cools below the melting point. Assuming planar regrowth from this Cr layer, the solidification velocity can be derived from the time-resolved resistivity data. Without this nucleation layer, we have previously seen significant liquid undercooling of thin Ni films prior to solidification, resulting in non-planar regrowth [12]. This layer also enhances the adhesion of processed films to the SiO_2 , allowing subsequent resistivity measurements.

Portions of the substrate were patterned for TCM (as described in reference [7]) photolithographically for post-deposition lift-off, in which selected regions of the wafer are covered with photoresist. After deposition of the metal film onto the photoresist-patterned substrate, these regions are chemically removed, leaving a thin film resistor of length 5.25 mm and width 75 μm . This sample geometry gives a good signal-to-noise ratio for the conductance measurement and allows a reasonably accurate determination of the specimen resistivity during the experiment. Isolated sections of the substrate (2 x 3 cm) were left unpatterned for XRD measurements.

Composition Determination

A section of the film deposited onto photoresist was retained for Rutherford Backscattering Spectrometry (RBS) to determine the composition and thickness (using 2.0 MeV incident α particles). Photoresist, consisting of light organic polymer molecules, only minimally interferes with the region of the RBS spectrum corresponding to Aluminum in the Ni_3Al layer; without it, the Si in the SiO_2 substrate would be superimposed on the Al peak. A density of 9.014×10^{22} atoms/ cm^3 was assumed for Ni_3Al . The resulting calculated composition, corrected for electronic screening [13], yielded a value of 72.1 at% Ni and a film thickness of 1500Å. The variation in both composition and thickness across the 5 cm substrate is expected to be small since the substrate-to-sources distance during the co-evaporation process was large ($\sim .75$ m).

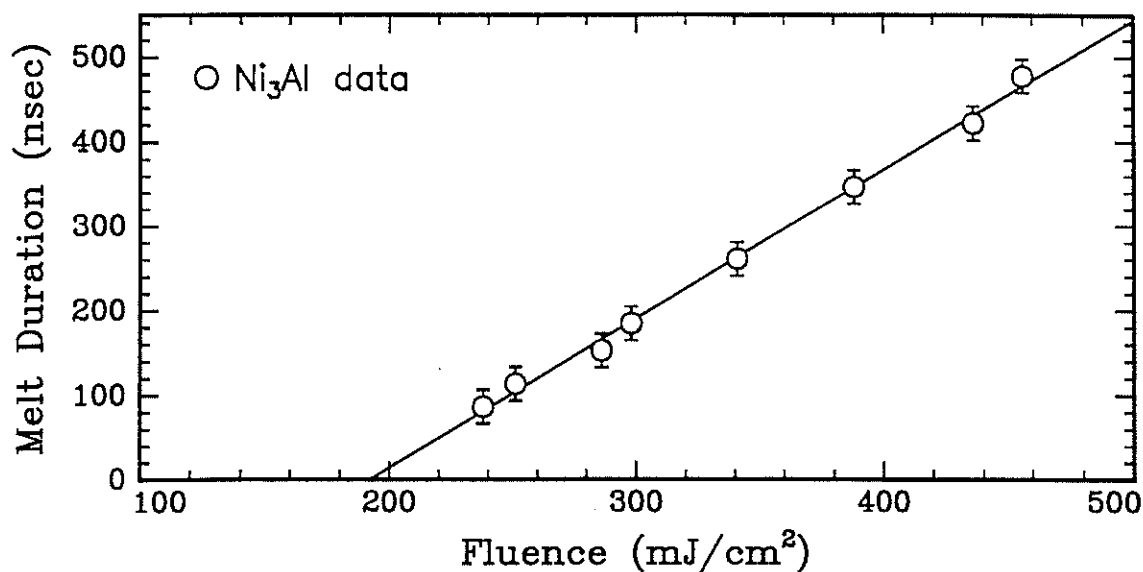


Figure 1. Melt duration versus incident XeCl fluence for a 1500Å Ni₃Al film. The substrate is a 1.0 µm thermally oxidized Si wafer which was coated with a thin layer of Cr to promote adhesion and planar solidification.

Pulsed Laser-induced Melting Procedure

A XeCl excimer pulse of wavelength 308 nm having a temporal duration of approximately 30 nsec FWHM, rendered spatially uniform by a homogenizer which splits the beam into 49 segments that are then recombined, was used to irradiate the film. Depending on the incident fluence, which was calibrated by comparing observed melt durations of bulk silicon with heat flow simulations [14], the film could be melted for periods in excess of 1 µsec. Figure 1 displays the observed melt duration as a function of the incident fluence. To minimize the time for which the liquid intermetallic was in contact with the Cr nucleation layer, a fluence of 285 mJ/cm², which provides a full-melt duration of only ~100 ns, was used to irradiate an unpatterned region of the wafer (~1 x 3 cm). RBS analysis shows little or no mixing of the Cr with the intermetallic after this brief melting, even after annealing at 600°C for 1 hr.

X-ray Diffraction

X-ray analysis was performed on a GE θ -2 θ diffractometer using white radiation from a Cr anode x-ray tube. A LN₂-cooled solid-state lithium-drifted silicon energy-dispersive detector was used to collect diffracted x-rays from the film, counting only x-rays with energies corresponding to the Cr K α peaks. The small volume of the film, as well as the characteristically weak nature of superlattice peaks, required long collection times (15 min/ 0.2° step in 2 θ). In this geometry, only crystals having a reciprocal space scattering vector normal to the film contribute to diffraction. Monitoring a superlattice and fundamental reflection pair with common scattering vector directions (i.e., (110) and (220)) guarantees that the same crystals are responsible for diffraction into both peaks, eliminating problems arising from possible texturing during any of the processing steps.

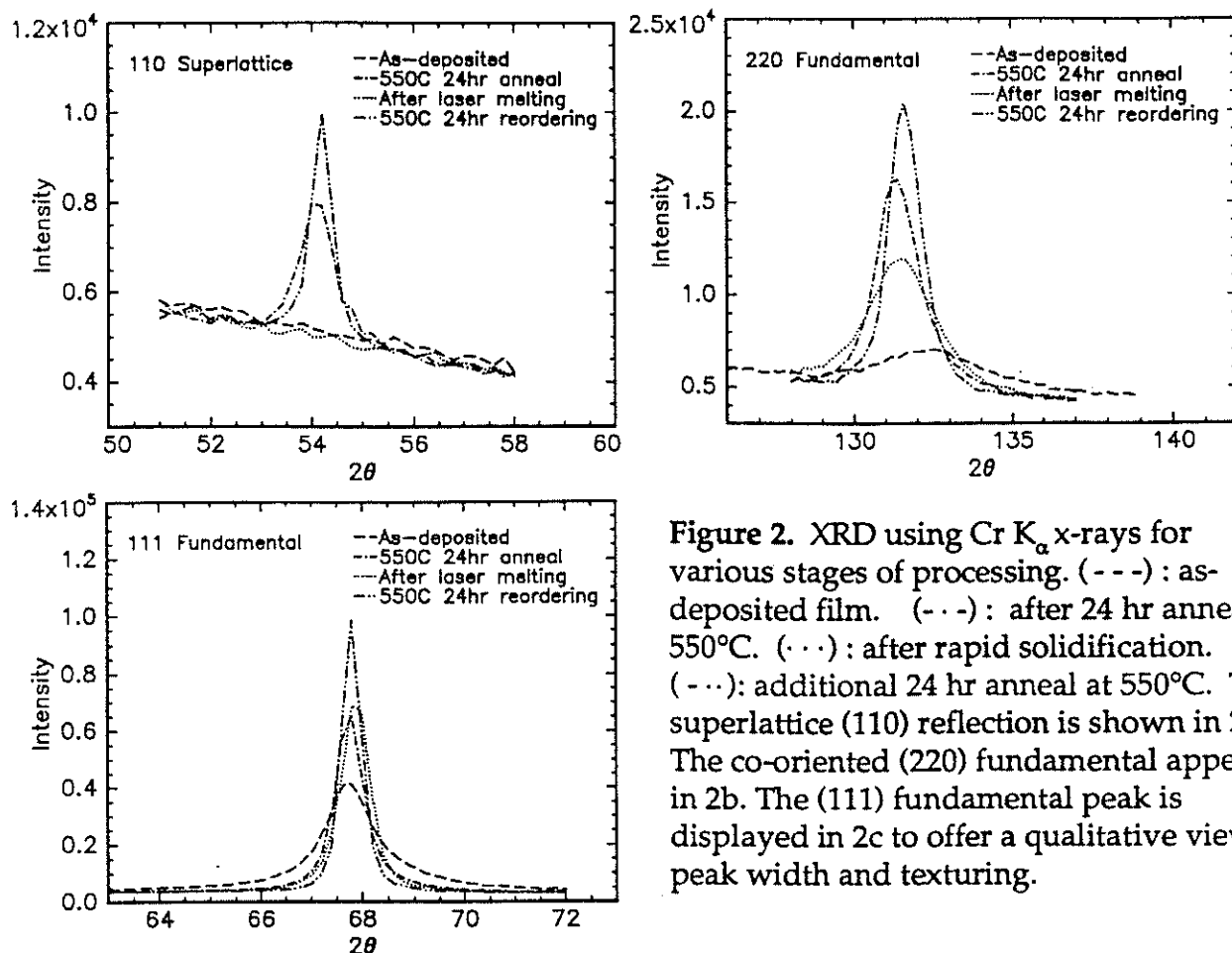


Figure 2. XRD using Cr K_α x-rays for various stages of processing. (---): as-deposited film. (- - -): after 24 hr anneal at 550°C. (...): after rapid solidification. (- · -): additional 24 hr anneal at 550°C. The superlattice (110) reflection is shown in 2a. The co-oriented (220) fundamental appears in 2b. The (111) fundamental peak is displayed in 2c to offer a qualitative view of peak width and texturing.

Figure 2 shows the resulting scans for the (110) superlattice, the (220) fundamental, and the (111) fundamental, after each step of the following sequence: as-deposited, vacuum (5×10^{-7} torr) furnace annealed at 550°C for 24 hrs, pulsed laser-induced melted and resolidified, and vacuum furnace annealed again at 550°C. The as-made deposit consists of crystals with diameter $\sim 150\text{\AA}$ and displays no observable superlattice peaks. TEM diffraction indicates a single phase fcc lattice and the peak widths in the XRD scans correlate well with the expected Scherrer broadening effect (predicted widths of $\Delta(2\theta)$ are 2.1° for the (111) peak and 4.3° for the (220) peak). After a 24 hr anneal of the as-made film, the (110) superlattice peak emerges and the fundamental peaks sharpen. TEM diffraction displays superlattice spots and a larger crystal diameter of $\sim 400\text{\AA}$. After quenching from the liquid, the superlattice disappears while the fundamentals remain, indicating a disordered fcc lattice. Subsequent annealing for 24 hrs at 550°C causes the (110) superlattice peak to reappear, indicating recovery of the ordered phase.

Resistivity Measurements

The TCM technique is essentially a transient resistivity measurement just before, during, and after the arrival of the excimer pulse. Assuming a linear expansion of 1.8% for the solid from room temperature to the melting point [15], and a 5% increase in thickness on melting, the liquid resistivity is fairly temperature independent at $\sim 96 \mu\Omega\text{-cm}$. A more accurate determination for this value awaits data for the high temperature

resistivity of the Cr nucleation layer, currently under investigation. The ratio between the resistivity of the liquid and the disordered solid at the melting temperature is ~ 1.14 . The resistivity of the disordered phase tends to increase as it cools, usually settling to $\sim 90 \mu\Omega\text{-cm}$.

Resistivity measurements have been made during subsequent annealing of the disordered state. The temperature coefficient of resistivity, defined by

$$\alpha = \frac{1}{\rho} \left(\frac{d\rho}{dT} \right)$$

is very small ($\sim 3.5 \times 10^{-5} \text{ K}^{-1}$) from 25-200°C for the disordered state. This corresponds well with the Mooij Criteria for concentrated disordered transition metal alloys which predicts that α depends only on the magnitude of ρ [16]. At 300°C, there is a noticeable drop in the resistivity ($\sim 1\%$) after an isothermal hold of 15 minutes (whereas a similar isothermal hold at 250°C indicates no change in resistivity). Cooling from this point results in a significant reduction in the resistivity which decreases nearly linearly with temperature and may be the effect of phonon scattering in the ordered γ phase. α increases by a factor of ~ 20 once this occurs, depending on the annealing temperature and time. The ordered phase has a slope of $\sim 0.050 \mu\Omega\text{-cm/K}$, close to the value of 0.057 reported for bulk material of composition 72 at% Ni [17]. The resistivity of the ordered film is $\sim 60 \mu\Omega\text{-cm}$ at room temperature, slightly higher than the bulk value of $53 \mu\Omega\text{-cm}$ extrapolated from data presented in reference [17]. The resistivity exhibits a strong dependence on composition and may be the source of the discrepancy.

The initial ordering reaction is apparently complete by 400°C (after a 15 minute isothermal hold at both 300° and 350°) since no further reduction in resistivity occurs for an isothermal hold of 15 minutes. An additional resistivity-lowering reaction appears near 450°C and may correspond to the initial stages of anti-phase boundary annihilation.

SUMMARY

The binary intermetallic compound Ni_3Al has been induced to solidify as a single-phase disordered fcc lattice following rapid solidification from an excimer laser-induced melt. The measured solidification velocity is $\sim 4 \text{ m/s}$. The disordered phase is metastable at room temperature, having a room temperature resistivity $\sim 50\%$ higher than that of the ordered phase and an extremely small temperature coefficient of resistivity. Ordering begins near 300°C during subsequent vacuum furnace annealing.

ACKNOWLEDGEMENTS

The authors are grateful to P.M. Smith and Dr. K-R Lee (Harvard) for valuable assistance in the pulsed laser melting lab set-up at Harvard, Prof. Eric Nygren (Ohio State) for helpful discussions concerning x-ray analysis, and Prof. M. O. Thompson (Cornell) for guidance in applying the TCM technique to metals. Support for this work was provided by the ONR Young Investigator Program (N00014-88-K-0548) and a grant from Sandia National Laboratories.

REFERENCES

1. R.W. Cahn, P.A. Siemers, J.E. Geiger, and P. Bardhan, *Acta. Met.*, **35**, (11), 2737, (1987).
2. R.W. Cahn in **High-Temperature Ordered Intermetallic Alloys, II**, edited by N.S. Stoloff, C.C. Koch, C.T. Liu, and O. Izumi (*Mat. Res. Soc. Proc.* **81**, Pittsburgh, PA 1987) p. 27.
3. J.D. Destefani, *Adv. Mat. & Proc.*, Feb., 1989, p. 37.
4. W. Boettinger and M.J. Aziz, *Acta. Met.*, **37**, (12), 3379 (1989).
5. A.R. Yavari and B. Bochu, *Phil. Mag. A*, **59**, (3), (1989), pp. 697-705.
6. R. Maurer, G. Galinski, R. Laag, and W.A. Kaysser in **High-Temperature Ordered Intermetallic Alloys, III**, edited by C.T. Liu, A.I. Taub, N.S. Stoloff, and C.C. Koch (*Mat. Res. Soc. Proc.* **133**, Pittsburgh, PA 1989) p. 423.
7. M.O. Thompson, G.J. Galvin, J.W. Mayer, P.S. Peercy and R.B. Hammond, *Appl. Phys. Letters* **42**, 445, (1983).
8. J.S.C. Chang and C.S. Koch, *J. Mater. Res.*, **5**, (3), 498-510, (1990).
9. C.L. Corey and D.I. Potter, *J. Appl. Phys.* **38**, 3894, (1967).
10. J.P. Clark and G.P. Mohanty, *Scripta Metall.* **8**, 959, (1974).
11. J.A. West, PhD Thesis, Harvard University, 1990.
12. H.A. Atwater, J.A. West, P.M. Smith, M.J. Aziz, J.Y. Tsao, P.S. Peercy, and M.O. Thompson (*Mat. Res. Soc. Proc.* **157**, Pittsburgh, PA 1989) p. 369.
13. J. L'Ecuyer et al., *Nucl. Instr. and Methods* **160**, 337 (1979).
14. M.J. Aziz, C.W. White, J. Narayan, and B. Stritzker in **Energy Beam-Solid Interactions in Transient Thermal Processing**, edited by V.T. Nguyen and A.G. Cullis, (*Editions de Physique*, Paris, France 1985) p. 231.
15. **Thermophysical Properties of High Temperature Solid Materials**, edited by Y.S. Touloukian, Thermophysical Properties Research Center, Purdue University (MacMillan Co., New York, 1967).
16. J. H. Mooij, *Phys. Stat. Sol A*, **17**, 521, (1973).
17. C.L. Corey and B. Lisowsky, *Trans. Met. Soc. AIME*, **239**, 241, (1967).